

In Situ Study of Water-Induced Segregation of Bromide in Bromide-Doped Sodium Chloride by Scanning Polarization Force Microscopy

Sutapa Ghosal,[†] Albert Verdaguer,[‡] John C. Hemminger,^{*,†} and Miquel Salmeron^{*,‡}

Department of Chemistry, University of California, Irvine, California 92697, and Materials Sciences Division, Lawrence Berkeley National Laboratory, University of California, Berkeley, California 94720

Received: August 19, 2004; In Final Form: January 12, 2005

The adsorption of water on Br-doped NaCl crystals has been studied in situ using scanning polarization force microscopy, a noncontact electrostatic atomic force microscopy operation mode. Both topography and contact potential images were acquired as a function of relative humidity at room temperature, from 0% to more than 55%. It was found that the surface of the freshly cleaved crystal has an inhomogeneous electrical surface potential distribution with the steps more negative than the terraces below 40% relative humidity. This difference disappears when the humidity reaches 40% and higher. Below 40% the step morphology experiences only small changes due to water adsorption; however, above 40% major changes take place due to solvation, segregation, and redistribution of lattice ions. Bromide-rich islands and crystallites segregate to the surface above 40% relative humidity followed by drying. These islands and crystallites have a negative surface potential relative to the rest of the surface. These effects are attributed to the preferential solvation and segregation of Br⁻ ions.

1. Introduction

Heterogeneous chemistry involving sea salt aerosols influences the chemical composition of the atmosphere.^{1–3} Reactions involving halogen anions at the surface of such aerosols have been proposed to be responsible for the release of reactive halogens into the troposphere.⁴ Bromide ions are a minor component of sea salt, the primary component being NaCl (Br/Cl ratio in seawater is only 1/660⁵). However, despite their low concentration in sea salt, bromide ions have been shown to play a disproportionately large role in tropospheric chemistry. Field as well as laboratory measurements indicate that the release of Br₂ and BrCl followed by photochemical production of Br is responsible for the localized surface ozone depletion observed over the Arctic at polar sunrise.^{6–8} The most likely sources of bromine in the Arctic environment are sea salt aerosols and/or seawater spray deposited on the surface of polar ice packs.⁹

The primary step in the activation of bromide in sea salt appears to involve halogen ions at an aqueous solution/air interface.¹⁰ Jungwirth et al.^{11,12} have carried out molecular dynamics simulations of a series of sodium halide solution/air interfaces. These simulations predict that all of the larger, polarizable halide anions are present at the interface, and bromide and iodide actually have higher concentrations in the interfacial region than in the bulk. In addition, their simulations support the segregation of the more polarizable Br⁻ ion relative to the Cl⁻ at the interface.¹¹ The greater propensity of bromide versus chloride at the interface of sea salt aerosols could explain the enhanced reactivity of bromide (despite its much lower concentration in seawater) in the Arctic during polar sunrise. Additionally, X-ray photoelectron spectroscopy (XPS) experiments on NaCl single crystals doped with low levels of bromide have demonstrated that the bromide ions segregate to the surface

following water vapor exposure.^{13,14} The segregation of bromide to the surface produces significant changes in the surface morphology of the crystal that have been observed using scanning electron microscopy.^{13,14}

One limitation of the above-mentioned XPS studies of Br segregation is that they are performed in high vacuum, where the water phase evaporates prior to surface analysis and therefore the experiment does not answer the question of whether surface enrichment of the anionic species is also true in the presence of water. It is therefore of great interest to examine this alkali halide–water system with in-situ techniques. Atomic force microscopies (AFM) are ideally suited for imaging surfaces with nanometer resolution. However, in the most standard operating modes of AFM the tip is in contact with the surface either continuously or intermittently and therefore is not suitable for imaging soft surfaces such as liquid-covered samples. To overcome this limitation, we have used a particular form of noncontact atomic force microscopy known as scanning polarization force microscopy (SPFM).^{15,16} SPFM uses electrostatic polarization forces that allow imaging at a distance of several hundred angstroms from the surface. This technique is particularly effective for imaging liquid-covered surfaces where large tip-to-sample distances are necessary to minimize perturbation of the surface. Another advantage of SPFM is that in addition to providing topographic images it allows mapping of the surface potential and ionic mobility on the surface.

Adsorption of water on various alkali halide surfaces has been studied previously using AFM and SPFM techniques.^{17–19} On the basis of the SPFM studies, a model was proposed to explain the adsorption of water and the ionic solvation processes taking place¹⁹ at the surface. According to this model, water adsorption on pure NaCl is characterized by two distinct relative humidity points, at 40% and 75% (the deliquescence point), which separate regions of different ionic mobility, surface potential, and morphology. For humidity values below 40%, the behavior of the crystal is dominated by water interaction with steps and leads to the preferential solvation of one of the ionic species.

* Corresponding authors. E-mail: jchemmin@uci.edu, salmeron@stm.lbl.gov.

[†] University of California, Irvine.

[‡] Lawrence Berkeley National Laboratory, University of California.

This produces changes in the contact potential distribution and in the ionic mobility. The changes are reversible, that is, upon drying, the original contact potential of the steps is recovered. Some topographic changes, including small displacements of the steps, however, are irreversible. Between 40% and 75% RH, both ionic species solvate at similar rates, leading to mass flow that is manifested in step motion. This process is irreversible, and both the step structure and the ionic distribution of the crystal surface are changed dramatically upon drying.

In this paper we present results from SPFM studies of humidity-induced bromide segregation in NaBr-doped NaCl-(100) (referred to as Br-doped) single-crystal surfaces. The results confirm previously reported water-induced bromide segregation and re-crystallization observed in Br-doped NaCl-(100) crystal surfaces using ex-situ X-ray photoelectron spectroscopy.¹³ Additionally, the present studies also provide an improved understanding of the structural modifications of the alkali halide crystal surfaces due to water adsorption.

2. Experimental Section

All the SPFM experiments were carried out at room temperature using a home-built AFM head and a commercial electronic control from RHK Technology, Inc. (STM 100). The microscope is housed inside a humidity-controlled glass bell jar equipped with two vacuum sorption pumps. A deionized water source was used to regulate the humidity in the bell jar. The water vapor pressure was monitored using a Baratron capacitance manometer. The relative humidity is therefore defined as the percentage ratio of the measured pressure to the saturation water vapor at room temperature. Within the bell jar, humidity could be regulated from 0% RH to almost 90% RH. Some experiments were also performed without evacuating the bell jar. In these cases, the humidity was controlled by circulating dry N₂ to decrease RH or by bubbling the N₂ through deionized water to increase the RH. The RH was measured using an Omega hygrometer. Since no differences were observed in the results obtained following either method, this will not be specified in the Results section.

The AFM was operated both in the standard contact mode and in the noncontact electrostatic mode (SPFM). Triangular-shaped boron-doped silicon cantilevers with a spring constant of 0.6 N/m were used for the experiments. In SPFM mode the oscillation amplitude was typically 1–2 nm, the image contrast did not change with amplitude in that range. The typical scanning speed was 1.56 ms/point.

A pure NaCl(100) single crystal and two Br-doped NaCl-(100) single crystals were obtained from the Crystal Growth Laboratory at University of Utah, Salt Lake City, Utah. The Br-doped crystals were grown from a melt of NaCl and NaBr. This method produces high-quality, uniformly doped crystals that are free of water impurities, in contrast to crystals grown from aqueous solution. The bulk compositions of the two Br-doped NaCl crystals were determined to have Br/Cl ratios of 0.07 and 0.001 by bulk elemental analysis.²⁰ All the samples were prepared by cleavage immediately prior to the experiment.

Operation of the AFM in the SPFM mode has previously been described in detail,^{15,16,21} and thus only a brief description is given here. In SPFM the image contrast is the result of electrical polarization forces between the tip and the sample surface. These forces are in the nano-newton range at tip–surface separations of a few tens of nanometers. A voltage consisting of a dc and an ac component of frequency ω (in the few kilohertz range) is applied to the conductive AFM tip, relative to a grounded support electrode. As a result of the electrostatic forces, the tip bends and oscillates. This oscillation contains several harmonics of the driving frequency. The second

harmonic is due to induced (polarization) charges. The first harmonic is due to fixed charges on the sample that determine the surface or contact potential. During imaging, the amplitude of the 2ω harmonic is detected and kept constant by feedback control of the tip–sample distance. This produces a “topographic” image, where the real topography is modulated by the local dielectric constant or polarizability. If the polarizability is constant the image is a true topography, as can be verified by comparing it with contact images acquired before or after the SPFM mode image. The first harmonic signal is obtained simultaneously with the topographic image and is used to null the contact potential by feedback to the dc component of the bias voltage, as in the Kelvin probe method. Separation of the two harmonic components is performed using two lock-in amplifiers and was demonstrated for the first time by Schönenberger et al.²² and Yokoyama et al.²³ Because of the feedback using the 2ω signal the topography is removed from the 1ω amplitude signal, which then provides an image containing only the contribution of contact potential.

3. Results

To compare the behavior of doped versus undoped samples we performed experiments on pure NaCl samples, on 0.1% Br-doped samples, and on 7% Br-doped samples. Pure NaCl, along with other alkali halides (KCl, KBr, and KF), was studied in the past using the SPFM technique.¹⁸ It was found that the mobility of surface ions, measured through the response of the ac lever oscillation amplitude to changes in the driving frequency, increases rapidly with humidity, a result attributed to the solvation by water of surface ions. It was also reported that the average potential of the surface increases, that is, it becomes more positive with increasing humidity, a result that was interpreted as due to preferential solvation of cations at low humidity, starting at step edges. The present results confirm the increase in ionic mobility with humidity, but disagree with the sign of the surface potential and its changes with humidity. We believe this to be in part due to differences in the history of previous exposures of the sample to water vapor. As we shall show, long exposure to ambient humidity higher than 40% can give rise to extensive surface ionic redistribution. The source of the salt crystals also appears to influence the observed surface potential behavior and this is likely due to the presence of impurities. The crystals used in this study were grown from a melt and are relatively free of impurities, while the previous results were obtained with commercially available crystals, which are known to contain impurities such as Ca.

3.1. Pure NaCl(100) Single Crystal. Figure 1 shows contact (top) and noncontact (middle) AFM images of the same region of a pure NaCl single-crystal surface cleaved under an ambient humidity of approximately 40% RH and then inserted into the chamber to be imaged at low humidity (11% RH). The surface is characterized by the presence of steps of monatomic (2.3 Å) and multiautomic height. The steps show some curvature, which is not evident in samples cleaved at low humidity (10% RH).¹⁹ As already known, the observed step curvature in Figure 1 is due to exposure to ambient humidity ($\geq 40\%$), which if prolonged for more than a few minutes induces step movement. The topographic resolution is higher in the contact image as compared to the noncontact SPFM image, as expected from the larger imaging distance (the tip is scanning at a height between 10 and 20 nm) in the SPFM mode, while in contact mode the contact radius (1–10 nm, depending on tip radius and load) determines the resolution. The simultaneously acquired surface potential image shows negative contrast at the step edges relative to the terraces. The value of the contact potential at the step

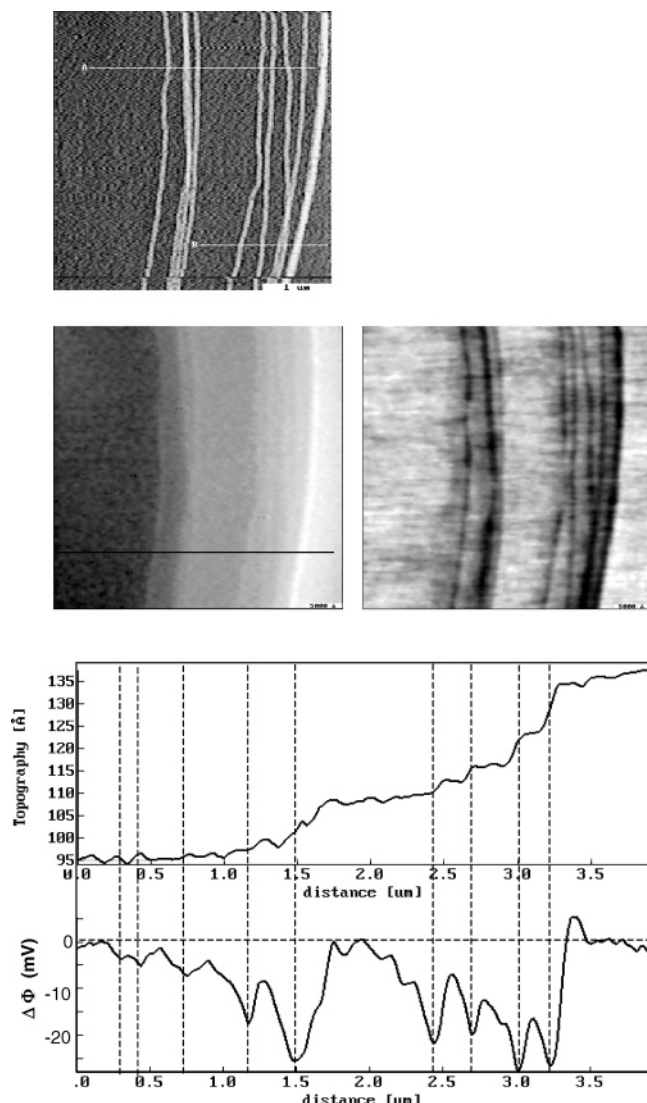


Figure 1. Top: Three-dimensional rendition of a $4 \times 4 \mu\text{m}$ contact AFM image of a pure NaCl single-crystal surface at low humidity (11% RH). Center: SPFM topography image (at 10 kHz) of the same area (left). Several monatomic steps (2.3 Å) are observed. The simultaneously acquired contact potential image is shown on the right side. Cursor profiles across the topographic and contact potential images are shown at the bottom.

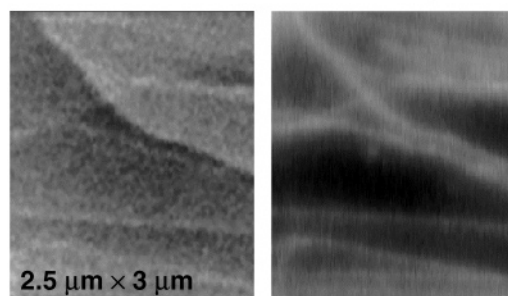
edges is of a few 10's of mV negative relative to the terraces. As the humidity increases the topography remains essentially unchanged while the contact potential difference between steps and terraces decreases. At 40% RH and above the contact potential contrast disappears and topographic changes occur in the form of rapid (in the scale of minutes and faster, depending on humidity) step displacements. The average contact potential of the surface is also found to decrease with increasing humidity.

As mentioned in the Introduction the observed contact potential changes are of opposite sign to those published earlier.¹⁹ One explanation for the discrepancy is the extreme sensitivity of the alkali halide surface structure (step morphology and ionic distribution) to water exposures. We found that only on crystals that have never been exposed to humidity above 40% (for NaCl) is the surface structure and surface potential reproducible upon humidity changes below 40%. If the crystal has been exposed to high relative humidity, either a long time at the boundary of 40% or for short times at higher values, substantial surface ionic displacements take place and the behavior of the surface potential afterward becomes unpredict-

NaCl

SPFM Topography

SPFM surface potential



KBr

Contact topography

SPFM surface potential

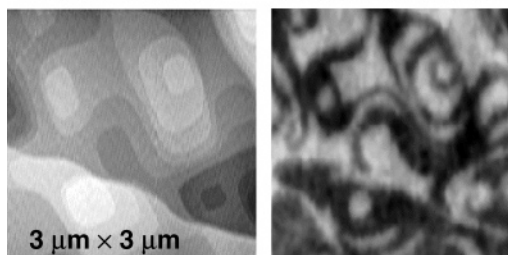


Figure 2. Ionic redistribution effects due to exposure to high humidity. Top: $2.5 \times 3 \mu\text{m}$ SPFM topography and surface potential images (using a 4 kHz ac-bias) of a NaCl crystal exposed to 45% RH for 10 min. Ionic redistribution produces regions with positive potential at the steps relative to the terraces, opposite to the observations at lower humidity (<40%) (Figure 1). Bottom: $3 \times 3 \mu\text{m}$ SPFM topography (left) and surface potential images (right) of a KBr crystal after exposure to 65% RH for 10 min followed by drying to 10% RH. The surface consists of multiple terraces separated by monatomic step. Ionic redistribution produced entire terraces and steps with opposite potential contrast.

able, with some steps and even entire terraces producing positive or negative potentials, due probably to small imbalances in the ionic distribution during surface recrystallization upon drying. This is shown in two examples in Figure 2. The top images correspond to SPFM topography (left) and surface potential (right) of a NaCl crystal that had been exposed for 10 min to 50% humidity prior to drying. The image shows the surface topography with steps and terraces, with positive potential values (+50 mV, approximately, relative to the terraces) at the step locations. Another dramatic example is shown in the two bottom images of the figure, corresponding to KBr. In this case, high humidity exposure (~10 min at 65% RH) prior to drying has resulted in a redistribution of ions that leave entire terraces and steps with opposite potential contrast, with differences of 35 mV between the dark areas and the bright areas. Given the observed impact of water vapor exposure on surface potential distribution, in the following experiments the water exposure history of the crystal was carefully controlled.

3.2. Br-Doped NaCl(100) Single Crystal. We found the results for the 0.1% Br-doped crystal to be very similar to those of the pure NaCl crystal, indicating that the 10^{-3} concentration of Br^- relative to Cl^- is not sufficient to produce appreciable changes under the water exposure regimes of these experiments. Therefore only the results obtained with the 7% doped crystal will be presented next.

Figure 3 shows contact and SPFM images of the 7% Br-doped NaCl(100) surface prepared by cleavage at 11% RH. At this humidity the topography is similar to that of the pure NaCl(100) surface. SPFM topography and surface potential images

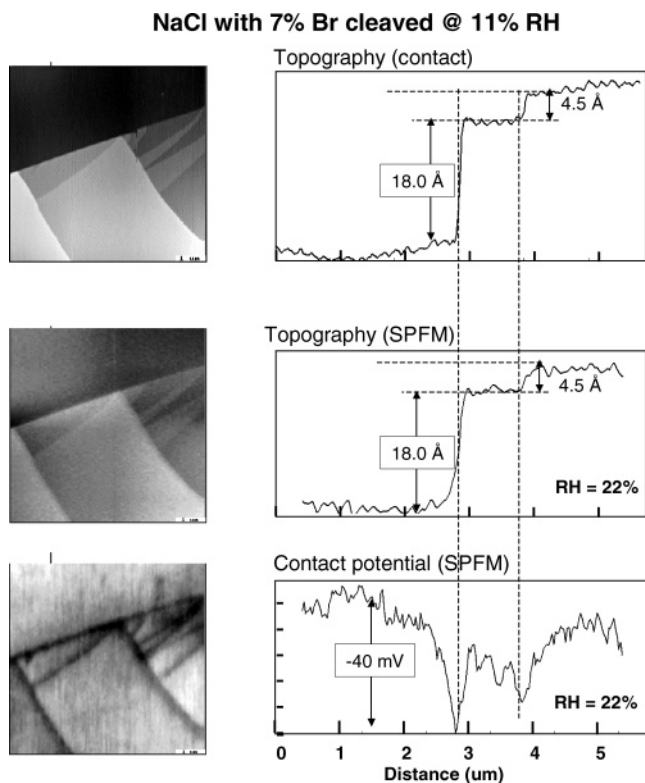


Figure 3. Top: $7 \times 7 \mu\text{m}$ contact AFM image of a 7% Br-doped NaCl(100) surface prepared by cleavage at 11% RH. Center: SPFM topographic image (4 kHz) of the same area acquired at 22% RH. The steps tend to be straight and aligned with the cubic axis crystallographic directions. Bottom: simultaneous SPFM surface potential image. The contact potential at the steps is more negative than on the terraces. This difference disappears when the relative humidity reaches 40%. The cursor profiles along the lines in the images are shown in the right side. The bottom terrace is separated by an 8-atom step (18 Å high) from a middle terrace, which is in turn separated by a 2-atom step (4.5 Å) from the upper terrace. The contact potential is negative at the steps relative to the terraces by about 40 and 28 mV, respectively.

of the same area were then acquired varying the humidity between 10 and 40% RH. An example corresponding to 22% RH is shown in Figure 3. The observed behavior is again similar to that of the pure NaCl, with negative contact potential at the step edges relative to the terraces provided that the humidity does not surpass 40%.

In case of the 7% Br-doped NaCl sample, exposure of the surface to 42% RH or above modifies the surface topography in a more profound way than for pure NaCl. This is shown in the images of Figure 4, acquired after exposure to 45% RH for 10 min followed by drying to 0% RH. Numerous small islands have been formed on the terraces in addition to the general rounding of steps observed also in pure NaCl. The small islands have irregular shapes and a height of $\sim 2.5 \text{ \AA}$ above the terrace, indicating one atomic layer thickness. Figure 5, shows the SPFM topography and KP images of another area. In the contact potential image the majority of the islands and the step edges are distinguished by a negative contrast (dark color in the image), which indicates that these islands and the step edges correspond to regions of negative surface potential relative to the terraces (the difference in potential between the dark and bright areas of the image is approximately -60 mV). If the humidity is increased again to 40%, the small islands disappear, although the larger step structures still remain visible.

3.3. Phase Separation and Recrystallization. The 7% Br-doped NaCl surface undergoes phase separation and recrystallization following exposure of the surface to 54% RH.

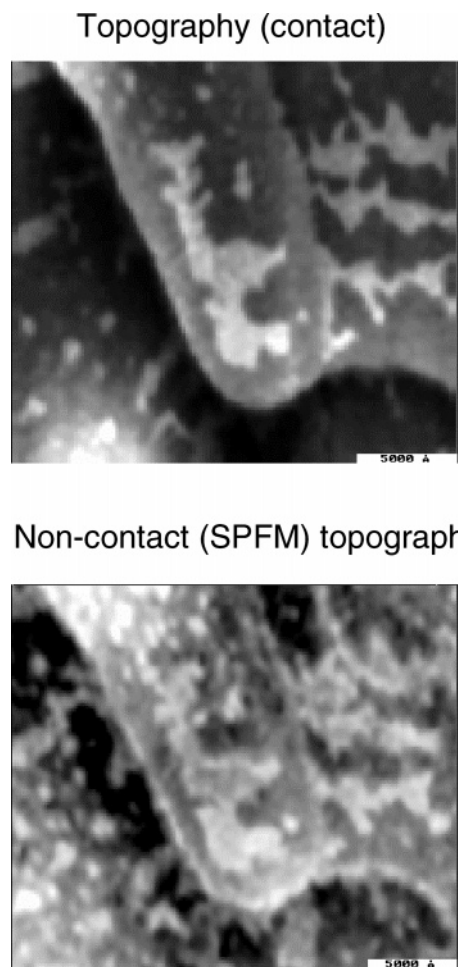


Figure 4. Top: $2 \times 2 \mu\text{m}$ contact AFM image of a 7% Br-doped NaCl(100) surface acquired after an exposure to 45% RH for 10 min followed by drying to 0% RH. Bottom: SPFM topography image (10 kHz) of the same area. Ionic redistribution effects occurring above 40% RH produce numerous irregularly shaped islands on the terraces in addition to the general rounding of steps. The height of the bright, irregular islands is 1 monolayer (2.3 Å).

As mentioned in the Introduction, the phase separation and growth of NaBr crystallites on the surface have been confirmed previously by SEM and EDX measurements.¹³ Figure 6 shows contact AFM (top) and SPFM topography (middle) and KP (bottom) images of the surface under dry conditions ($\sim 0\%$ RH) following an exposure to 54% RH for 30 min. Crystallites decorating the surface, particularly along the step edges, are clearly visible in both the contact and noncontact images. The average height of the crystallites is $\sim 35 \text{ \AA}$. The bottom image shows the corresponding contact potential. As can be seen, the crystallites correspond to regions of negative surface potential, as in case of the monolayer islands formed following exposure to 45% RH on the freshly cleaved surface discussed above.

4. Discussion

The results presented above indicate that the Br-doped NaCl surfaces behave similarly to those of pure NaCl when the relative humidity is below 40% on virgin surfaces, that is, on surfaces that have never been exposed to water vapor above that humidity value. In both cases there is an excess of negative potential associated with step edges that indicate the presence of a negative dipole in that region. The average surface potential becomes more negative with increasing humidity. This could be due to water-induced restructuring of the surface, for

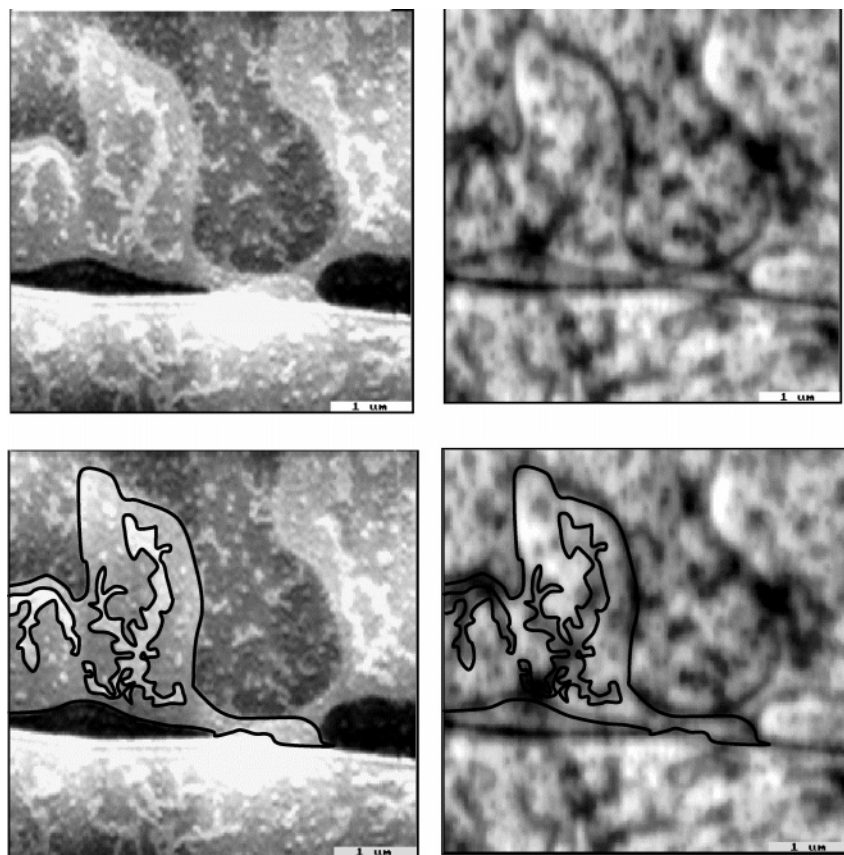


Figure 5. Top: $5 \times 5 \mu\text{m}$ SPFM topography (left) and surface potential images (right) (10 kHz) of a 7% Br-doped NaCl(100) surface acquired after exposure to high humidity conditions (40% RH) for a few minutes followed by drying to 0% RH. Bottom: Same images with some of the steps and islands outlined for clarity. In the surface potential image, the islands and the step edges are distinguished by a negative contrast (dark color in the image).

example, anions being pulled upward from their sites at low humidity, and to the preferential removal of anions from the lattice at higher humidity, starting at steps. These anions then become solvated and mobile. This mobility was studied in detail in our previous work by measuring the frequency dependence of the polarization force.^{19,24} As the humidity increases, the spatial distribution of solvated anions changes due to their increased mobility until the concentration at the terraces equals that at the steps. This results in the disappearance of contact potential contrast around 40% between terraces and steps. At higher humidity, increased ionic mobility leads to rapid motion of the steps.

While similar events occur on both pure and Br-doped NaCl, the rearrangements observed on the doped surface are much more extensive. For example, the numerous irregular islands on the terraces in Figures 4 and 5 are observed only on the Br-doped samples. We can understand the origin of this behavior by considering the lower deliquescence point of NaBr (58% RH) as compared to that of NaCl (75%) which indicates that solvation of Br^- is faster than that of Cl^- for similar relative humidity conditions. The faster solvation of Br^- ions would result in efficient lattice removal and mobility of surface Br^- ions above 40% RH, thereby exposing Br^- ions in the second layer that could in turn solvate, enriching the surface in Br^- . According to this model, enhanced mobility of Br^- ions above 40% RH would result in their segregation to the surface. The segregated ions would aggregate and form areas rich in Br^- relative to Cl^- such as the islands decorating the 7% Br-doped NaCl surface following exposure to relative humidities $>40\%$. This model is in agreement with the observation of surface

enrichment of Br^- by XPS¹³ following exposure to relative humidities above 40%.

The negative contrast of the Br^- -rich islands is again explained by the preferential solvation and segregation of Br^- , as a result of the lower deliquescence point of NaBr. For the same relative humidity, more anions are solvated or displaced from their lattice positions at the surface of the Br^- -rich islands than on the rest of the crystal surface, thus giving rise to a negative contact potential relative to the terraces.

The formation of crystallites that decorate the steps and terraces (Figure 6) after exposure to high humidity (13 Torr of water vapor $\sim 54\%$ RH) followed by drying can be understood by the larger size of the Br^- ion (196 pm ionic radius)²⁵ relative to that of Cl^- (181 pm ionic radius)²⁵ that leads to a lattice mismatch relative to the NaCl lattice underneath, so that upon drying the mobile ions segregate to form Br^- -rich crystallites.

As mentioned above, the 0.1% Br-doped NaCl produced results similar to those of the pure NaCl. The difference in surface morphology between the 0.1% and 7% doped samples is likely due to the large difference in Br^- content, close to 2 orders of magnitude between the two samples. As a result, the impact of Br^- segregation on surface morphology is likely to be quite different in these two samples.

5. Conclusions

By using atomic force microscopy in a noncontact electrostatic mode (SPFM), we confirmed previous reports of water-induced bromide segregation and re-crystallization in Br-doped NaCl(100) crystal surfaces obtained using ex-situ X-ray photoelectron spectroscopy.¹⁹ In addition, the new SPFM results

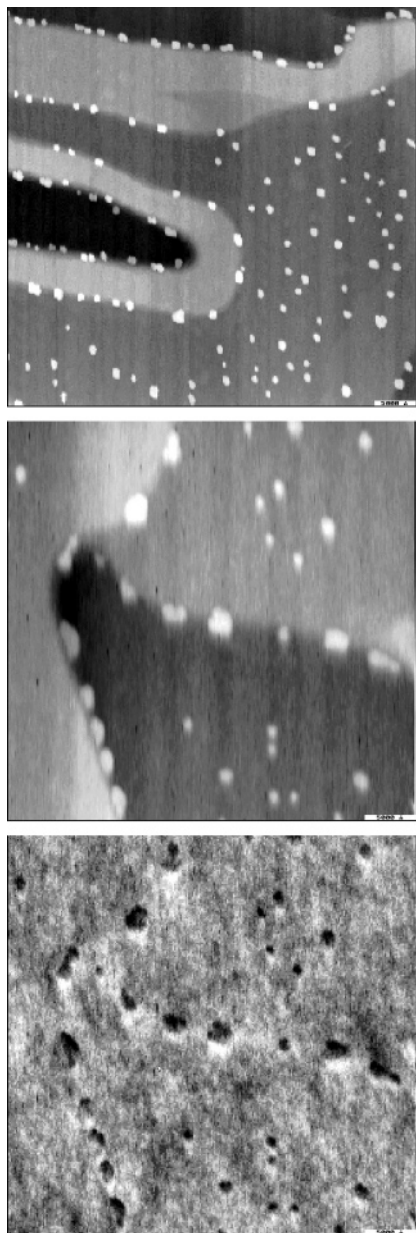


Figure 6. Top: $5 \times 5 \mu\text{m}$ contact AFM image of the 7% Br-doped NaCl(100) surface under dry conditions (0% RH) following an exposure to 54% RH for 30 min. Center: $4 \times 4 \mu\text{m}$ SPFM topography image (10 kHz) of the 7% Br-doped NaCl(100) surface under dry conditions (0% RH) following exposure to 54% RH for 30 min. Bottom: SPFM surface potential image of the same area acquired simultaneously. The crystallites correspond to regions of negative surface potential.

provide an improved understanding of the structural modifications of the alkali halide crystal surfaces due to water adsorption. They indicate that surface modification by water is initiated at step edges, which become negatively charged. We interpret this result as an indication of preferential solvation of anions. It is quite likely that the selective segregation of bromide observed in Br-doped NaCl crystal is also true for sea salt aerosols/particles under ambient relative humidity conditions, which are

frequently above 40%. This preferential segregation of bromide would then influence the availability of sea salt bromide for atmospherically relevant heterogeneous reactions, such as the Br-catalyzed destruction of ozone during Arctic sunrise. Hence, any modeling of Br chemistry involving sea salt should incorporate the segregation phenomena described here.

Acknowledgment. This work was supported by the Director, Office of Energy Research, Office of Basic Energy Sciences, Materials Science Division, of the U.S. Department of Energy under Contract No. DE-AC03-76SF00098. S.G. and J.C.H. acknowledge support from the National Science Foundation under Grant ATM-0080806, a Collaborative Research in Chemistry Grant, CHE-0209719 and the NSF Supported Environmental Molecular Sciences Institute at UCI (CHE-0431312). S.G. is grateful to Hendrik Bluhm for his help and guidance with the SPFM instrumentation. A.V. acknowledges a postdoctoral fellowship from the Spanish Science and Education Ministry.

References and Notes

- (1) Ravishankara, A. R. *Science* **1997**, *276*, 1058.
- (2) Andreae, M. O.; Crutzen, P. J. *Science* **1997**, *276*, 1052.
- (3) Finlayson-Pitts, B. J.; Hemminger, J. C. *J. Phys. Chem. A* **2000**, *104*, 11463.
- (4) Knipping, E. M.; Lakin, M. J.; Foster, K. L.; Jungwirth, P.; Tobias, D. J.; Gerber, R. B.; Dabdub, D.; Finlayson-Pitts, B. J. *Science* **2000**, *288*, 301.
- (5) *Handbook of Chemistry and Physics*; CRC Press: Boca Raton, FL, 1990–1991; 14 pp.
- (6) Oum, K. W.; Lakin, M. J.; Molina, M. J.; Finlayson-Pitts, B. J. *Geophys. Res. Lett.* **1998**, *25*, 3923.
- (7) Koop, T.; Kapilarshrami, A.; Molina, L. T.; Molina, M. J. *J. Geophys. Res.* **2000**, *105*, 26393.
- (8) Foster, K. L.; Plastringer, R. A.; Bottenheim, J. W.; Shepson, P. B.; Finlayson-Pitts, B. J.; Spicer, C. W. *Science* **2001**, *291*, 471.
- (9) Barrie, L. A.; Platt, U. *Tellus* **1997**, *49B*, 450.
- (10) Hunt, S. W.; Roeselová, M.; Wang, W.; Wingen, L. M.; Knipping, E. M.; Tobias, D. J.; Dabdub, D.; Finlayson-Pitts, B. J. *J. Phys. Chem. A* **2004**, *104*, 11463.
- (11) Jungwirth, P.; Tobias, D. J. *J. Phys. Chem. B* **2002**, *106*, 6361.
- (12) Jungwirth, P.; Tobias, D. J. *J. Phys. Chem. B* **2001**, *105*, 10468.
- (13) Ghosal, S.; Shbeeb, A.; Hemminger, J. C. *Geophys. Res. Lett.* **2000**, *27*, 1879.
- (14) Ghosal, S. *Role of Water in Alkali Halide Heterogeneous Chemistry Relevant to the Atmosphere – A Surface Science Study*. Ph.D. dissertation thesis. University of California, Irvine, Irvine, 2001.
- (15) Hu, J. X.-d.; Ogletree, D. F.; Salmeron, M. *Science* **1995**, *268*, 267.
- (16) Hu, J. X.-d.; Ogletree, D. F.; Salmeron, M. *Appl. Phys. Lett.* **1995**, *67*, 476.
- (17) Shindo, H. O. M.; Baba, K.; Seo, A. *Surf. Sci.* **1996**, *111*, 357–358.
- (18) Dai, Q. H. J.; Salmeron, M. *J. Phys. Chem.* **1997**, *101*, 1994.
- (19) Luna, M.; Rieutord, F.; Melman, N. A.; Dai, Q.; Salmeron, M. *J. Phys. Chem. A* **1998**, *102*, 6793.
- (20) Desert Analytics POB, Tucson, AZ 85717.
- (21) Hu, J.; Salmeron, M. Studies of wetting and capillary phenomena at nanometer scale with scanning polarization force microscopy. *Nano-Surface Chemistry*; Rosoff, M., Ed.; Marcel Dekker: New York, Nov. 1, 2001; Chapter 6, pp 243–287.
- (22) Schönenberger, C.; Alvarado, S. F. *Phys. Rev. Lett.* **1990**, *65*, 3162.
- (23) Yokoyama, H. J.; Inoue, T. *Jpn. J. Appl. Phys., Part 2* **1993**, *32*, L1845.
- (24) Xu, L.; Salmeron, M. *Langmuir* **1998**, *14*, 5841.
- (25) Atkins, P. W. *Physical Chemistry*, 3rd ed.; W. H. Freeman and Company: New York, 1986.